Transactions of the **14th International Conference on Structural Mechanics in Reactor Technology** (SMiRT 14), Lyon, France, August 17-22, 1997 **HKW/6**

Non-linear analysis of the seismic shear wall ISP using a simplified-finite-element code

Mazars J., Ghavamian Sh.
ENS Cachan / LMT, France

ABSTRACT

The work under taken in this study was to reproduce by numerical modeling, model tests carried out by the Japanese organization NUPEC on the Tadotsu shaking table. Experiments where reinforced concrete box-like walls that had under gone different levels of seismic excitations, reaching their ultimate resistance at the end. This paper illustrates calculations done at LMT Cachan in order to simulate the complex non-linear behavior of these structures, using a simplified-finite-element code specially adapted for reinforced concrete structural analysis.

INTRODUCTION

The safety assessment of nuclear reactor buildings can not be achieved if the ultimate strength of its constituents are not well evaluated. "Structural walls" participating as horizontal resisting elements determine the capacity of a building against earthquakes. That is why since 1986 Nuclear Power Engineering Corporation (NUPEC) launched a wide and deep project to improve and develop seismic safety evaluation methods concerning these type of structures. As a part of this program a series of shaking table experiments have been conducted on two similar squat shear walls, with loadings ranging from very low to very high excitation levels bringing them to their ultimate capacity.

Following this experimental campaign, the data has been opened to the international scientific and industrial community within the framework of a benchmark proposed by NUPEC and sponsored by OECD/NEA/CSNI, named SSW-ISP (Seismic Shear Wall Standard Problem).

We at LMT Cachan, as a member of the French research network GEO, participated in this benchmark, and have conducted analyses on all steps of the experiment. This work is about analyses undertaken using a simplified-finite-element method, taking into account shear effects, and including a concrete constitutive modeling, based on damage concept and crack closure aspects.

At the beginning, using enriched beam elements to describe shear walls dynamic behavior brings up many questions. This is why during the process of this benchmark, we at LMT Cachan, also took advantage of some other analyses carried out in the framework of GEO French team (CEG-DGA-INSA Lyon). These analyses were made using more sophisticated 2D and 3D codes, necessary to study the influence of out of plane mechanism which might have been activated during a real experimental situation. But obviously using beam elements

may not describe high non linearities, such as bond failure specific to shear walls, unless more enriched.

EXPERIMENTAL ASPECTS

Two identical specimens were used for this campaign. Each was constituted of a shear wall with flanges at it sides, and anchored to two top and base slabs. Since these were scaled mock-ups, additional weights were also added to the top slab in order to create a vertical stress close to a real situations. Figure 1 illustrates some details about their geometrical features, while material characteristics and structural properties are summarized in table 2.

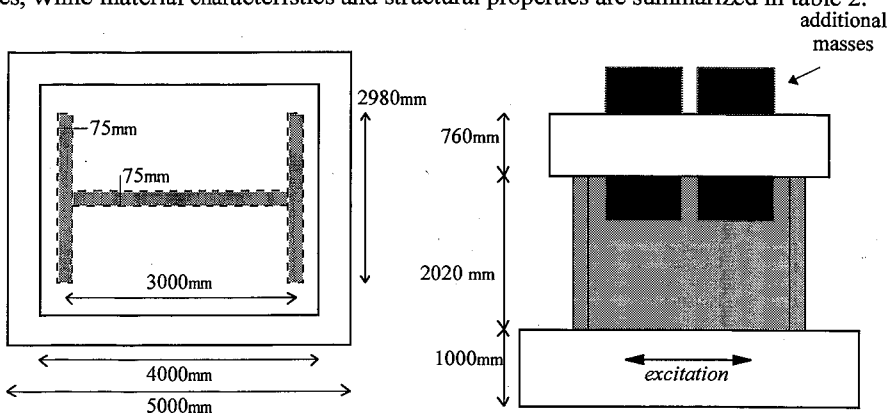

Figure 1, Geometrical features of specimens

Web wall cross section surface	m^2	0.225
Flange wall cross section surface	m^2	0.596
Vertical reinforcement ratio	%	1.2
Horizontal reinforcement ratio	%	1.2
Compressive concrete strength	MPa	28.6
Concrete Young's modulus	MPa	22 960
Reinforcement yield strength	MPa	384
Total masse of upper region (slab + add. masses)	t	(29.1+92.9)=122.0
Vertical stress in the walls	MPa	1.5

Table 2, Material and structural characteristics

Base slabs of specimens were anchored to the table and motions were only in one direction, parallel to the web wall. The loading program was constituted of 6 vibration steps. The same input signal, with an increasing amplitude, was used throughout the steps. Table 3 indicates these steps and their excitation intensities. The duration of the signal was 12 seconds for each vibration step.

Vibration step	Run-1	Run-2	Run-2d	Run-3	Run-4	Run-5
Input acceleration (m/s^2)	0.530	1.120	3.040	3.520	5.770	12.300

Table 3, Vibration steps

Pre-excitations of very low intensities were also added to each vibration step. In this way dynamic characteristics of the structures (first natural frequency and equivalent damping ratios) could be measured. Table 4 shows these results. The behavior of the structure

remained nearly linear under Runs 1 and 2. Run 2d was then added to the initial vibration program to make the transition into non linearities. That is why for these first 3 Runs only one natural frequency is given.

Vibration step	Run-1	Run-2	Run-2d	Run-3	Run-4	Run-5
1 st natural frequency (Hz)	13.2	-	-	11.3	9.0	7.7
Equivalent damping ratio (%)	1.1	-	-	2.5	3.0	4.0

Table 4, Dynamic characteristics measured before each Run (specimen 1)

Among different experimental data, figure 5 shows maximum horizontal-inertial-force versus maximum horizontal relative displacement (between top and base). These were obtained from time history records of each vibration step. One can notice the nonlinear behavior of the specimen for Runs 3, 4 and 5, and linear elastic for other first 3 Runs.

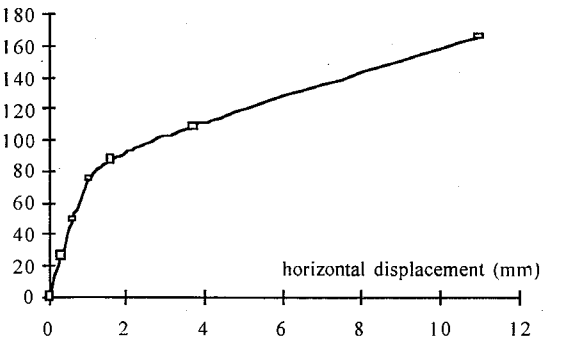

Figure 5, Horizontal maximum inertial force versus relative top slab displacements

DESCRIPTION OF MATHEMATICAL TOOLS

Computer code

To simulate the nonlinear behavior of the RC specimen we used a simplified finite element code, named EFiCoS. Using Newmark's integration method and Newton-Raphson algorithm to deal with non-linearities, this code has been enriched during the last years by different researchers at our laboratory. It is a displacement based finite element code using multilayered beams to represent structural elements. A transversal description of a beam element is shown on figure 6, where different layers of concrete (some containing reinforcement steel) can undergo material nonlinearities. A mixed-law, governs homogenized layers constituted of two superposed materials, concrete and steel [1].

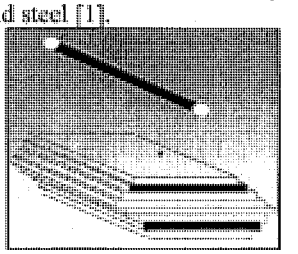

Figure 6, A multi layered beam element

The use of a multi layered finite element configuration was adopted to limit the size of the problem which provides a compromise between a very fine modeling of the structure which is costly and a cheaper coarse modeling which may not provide sufficient local information. Other advantage is the simplicity of uniaxial behavior for its constituting cross sectional layers (or enhanced uniaxial behavior to include shear as one can see below), while providing sufficient local information.

Constitutive law of concrete

Seismic loading, which includes cyclic aspects, produce microcracking in concrete with the following effects : - material stiffness loss as microcracks open,
- stiffness recovery when cracks close again.

To simulate this behavior we used a damaged model [2], which incorporates two scalar damaged variables, one damaged due to tension D_1, the other damaged due to compression D_2, which includes a stiffness recovery procedure and the description of anelastic strains (equations 1 to 3). Figure 7, shows a typical stress-strain diagram for this constitutive law of concrete under a tension compression cycle of loading.

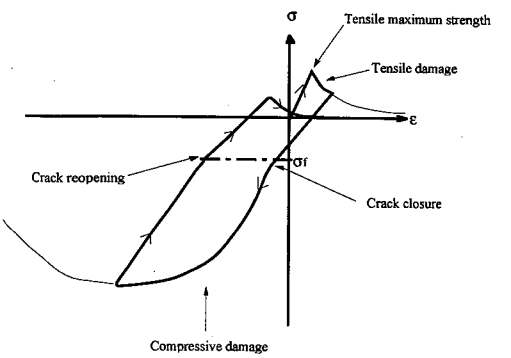

Figure 7, Nonlinear uniaxial stress-strain diagram for concrete

$$\underline{\varepsilon} = \underline{\varepsilon}^e + \underline{\varepsilon}^p = elastic + permanent,\ strains \tag{1}$$

$$\underline{\varepsilon}^e = \frac{\underline{\sigma}^+}{E_0(1-D_1)} + \frac{\underline{\sigma}^-}{E_0(1-D_2)} + \frac{\nu}{E_0}(\underline{\sigma} - Tr\underline{\sigma}\underline{1}) \tag{2}$$

$$\underline{\varepsilon}^p = \frac{\beta_1 D_1}{E_0(1-D_1)} \frac{\partial f(\underline{\sigma})}{\partial \underline{\sigma}} + \frac{\beta_2 D_2}{E_0(1-D_2)} \underline{1} \tag{3}$$

E_0 is the initial Young's modulus, ν is the Poisson ratio.
$\underline{\sigma}^+$ and $\underline{\sigma}^-$ are respectively the "tensile-tensor" and the "compression-tensor".
D_1 and D_2 are respectively the damage variables for tension and compression.
β_1 and β_2 are constants and $f(\underline{\sigma})$ allows to manage the crack closure.
Where damage parameters D_1 and D_2 change when a local elastic energy based criteria is reached.

An important feature of the beam formulation implemented in this code is its capacity to take into account shear strains. Classically, the formulations for a beam element are based on the assumption that plane sections remain plane, and then considering a uniaxial behavior of each layer. But this is no longer satisfactory when shear strains have to be encountered. Here shear strains are considered by :

- first, introducing the tensor relation given in (4), and then considering relation (1) we obtain a mean strain value ε_{12}, assuming Bernoulli plane section assumption. This is then enriched with a kinematics relation issue from Timoshenko works [3], and continued by Crisfield [4].

$$\begin{pmatrix} \varepsilon^e_{11} \\ \varepsilon^e_{12} \end{pmatrix} = \begin{bmatrix} \frac{1}{E_D} & 0 \\ 0 & \frac{1}{E_D} + \frac{\nu}{E_0} \end{bmatrix} \begin{pmatrix} \sigma_{11} \\ \sigma_{12} \end{pmatrix} \tag{4}$$

$$\varepsilon_{12}(y) = \varepsilon_{12m} + g(y) \tag{5}$$

With $E_D=E_0(1-D_2)$ when $\sigma=\sigma^-$, or $E_D=E_0(1-D_1)$ if $\sigma=\sigma^+$.

In an elastic formulation, this results in a parabolic distribution of the shear strains (5). We then admit that this remains acceptable for an elastic damagable behavior.

For more details the reader is invited to consults the documents in reference [5, 6].

STRUCTURAL MODELING

First modeling

Walls were modeled using 9 beam elements (constituted of 46 layers each), while top slab and additional masses were geometrically concentrated at their respective center of gravity along the height at the structure (see figure 8). For the first modeling, an assumption was made for the base condition as perfectly anchored to the ground (shaking table considered inflexible). So the accelerations recorded an the upper surface of the base slab were used as the input motion for the analysis.

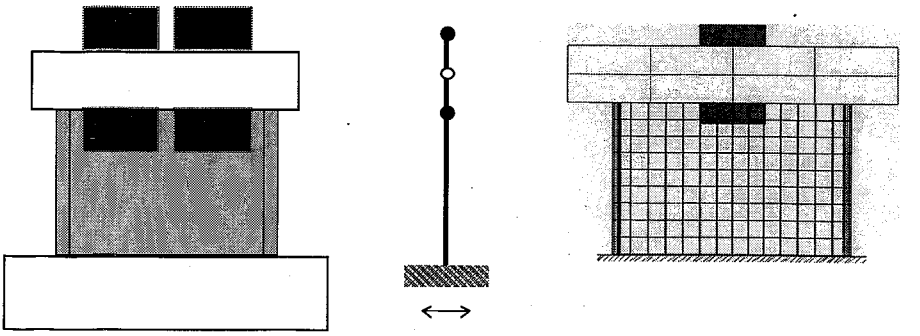

Figure 8, First mechanical modeling, and the finite element mesh

Meanwhile, values obtained from mechanical properties of materials (see table 2) were directly taken into account without any further assumptions. A Rayleigh proportional viscous damping at 2% was calculated at the beginning of the analysis. Damping constants were calculated considering first two natural frequencies, in the plane containing the vibration. This was then used through out the entire analysis at all steps without any updating.

Boundary conditions adjustment

Responses obtained after the first analysis were then compared to the experimental time history data. Different observations could be made for each Run. Regarding elastic and nonlinear time history displacements and accelerations two major remark were made :

1- For Run-1, great differences can be seen for amplitudes, but even more on the periods,
2- Some discrepancies over nonlinear responses of Runs 4 and 5.

We had detected that the first natural frequency of the F.E. model was higher than the experimental one, by 15%. Since masses were most correctly introduced in the model, the only possibility to lower this frequency was to reduce the global stiffness of the structure. This could be achieved in two ways : changing material stiffness or the boundary conditions.

A decrease in material stiffness could be justified by microcracked concrete, present even at very low vibration loads. To change boundary conditions it should be assumed that the base of the mock-up is not a perfect anchor. Which is mostly the case in real experimental situations.

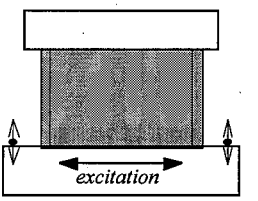

Figure 9, Location of vertical acceleration sensors.

The choice we made was to modify boundary conditions. In fact during further observations of experimental data we found that vertical acceleration sensors had recorded non negligible accelerations at the upper surface of the base slab (figure 9). Vertical accelerations recorded by two sensors placed at each side of the model had recorded showed signals totally out of phase (π) meaning that the base of the structure was undergoing rotations.

This could be attributed to many different sources ; deformation of the base slab, deformation of high strength steel bars used to anchor the slab to the shaking table, deflection of the shaking table. Unfortunately no accelerations were measured at the surface of the table. That is why we adopted the choice to wrap-up all different sources into an elastic-linear flexible base element, using a new finite element beam. Figure 10 shows the mechanical scheme of this modeling.

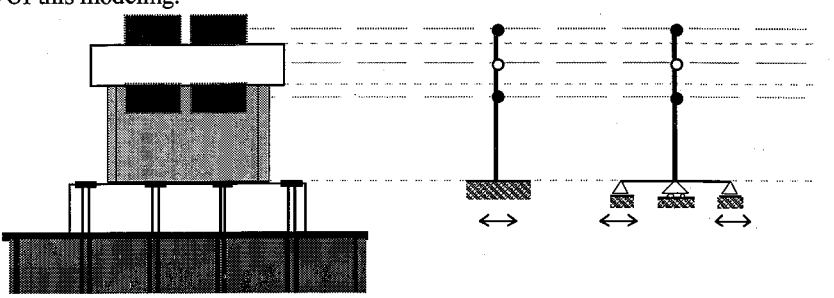

Figure 10, Mechanical scheme of the first and the final F.F modeling

Then the stiffness of this base element was calculated so that the first natural frequency of the modeling was the same as the experimental one measured before Run-1 (13.2 Hz). No further adjustments were made for other Runs. Table 11 shows the comparison of the first natural frequencies.

Structures	Modeling Anchored base	Modeling Semi-rigid base	Experimental specimen
1st natural frequency (Hz)	14.7	13.2	13.2

Figure 11, Mechanical scheme of the first and the final F.F modeling

FINAL RESULTS

Calculations made with the new modeling gave closer results to experimental data. Figure 12 are time history comparisons for Run-4 [7].

While this time for Run-1 the periods were found to be in well agreement with the experiment, amplitudes were higher. This can mostly be attributed to the high sensitivity of results to the way damping is modeled. For Run-4 responses matched very well in frequency and amplitude. Residual displacements were also found to be well determined.

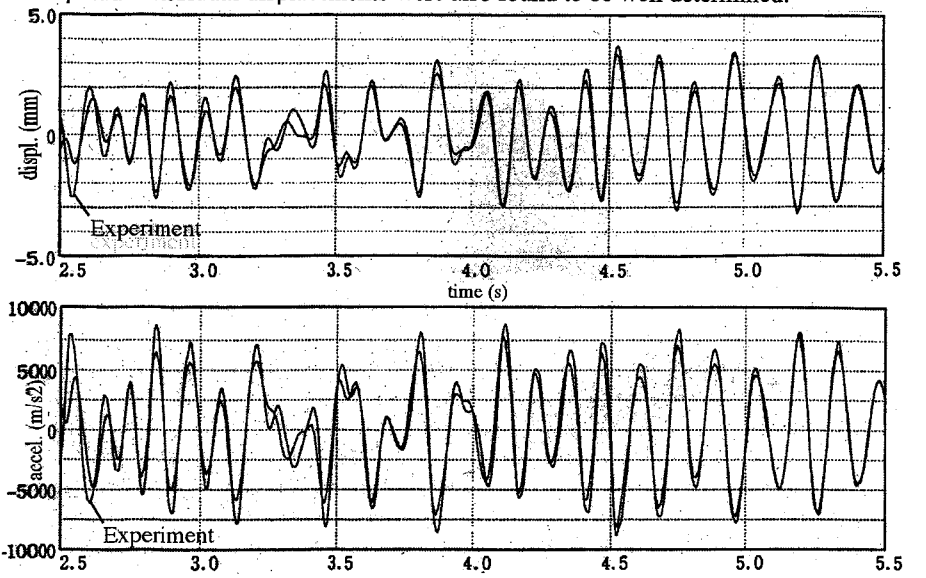

Figure 12, Horizontal displacement and top slab acceleration comparisons for Run-4

In table 13 one can compare frequency evolution from the experiment and analysis. Maximum responses obtained from all Runs are also compared for the horizontal inertial force versus top slab displacement (figure 14).

		RUN-1	RUN-2	RUN-2d	RUN-3	RUN-4	RUN-5
Exp.	(Hz)	13.2	13.2	13.2	11.3	9.0	7.7
EFiCoS	(Hz)	13.2	13.1	13.1	11.6	11.0	6.5

Table 13, Frequency evolution, comparison between experiment and analysis

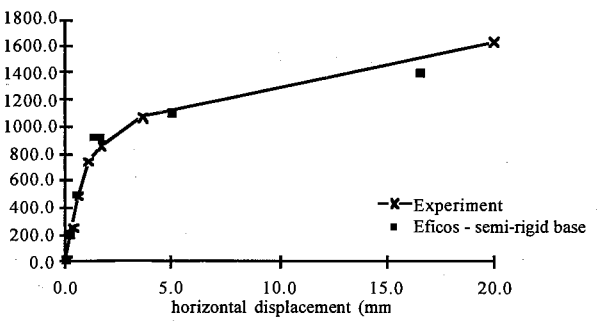

Figure 14, Maximum envelope responses

Other results such as those concerning the natural frequency evolution of the structure caused by the stiffness degradation of the concrete and yielding of vertical reinforcements are available and will be presented at the conference.

CONCLUSIONS

Usually the lack of information concerning the non-linear behavior of concrete makes it difficult to calibrate sophisticated constitutive law modeling. Never the less in this study we used usual parameters classically employed for normal concrete, with no specific modifications. However, damage concept allows a well description of gradual stiffness degradation of the material. Which is essential in nonlinear transient dynamic analysis.

Another major uncertainty, usually presented in structural dynamics, concerns the real boundary conditions. However perfect, no boundary condition may be considered such. In this study, describing all possible sources responsible for the base rotations would have been a tedious task (even if informations were available). But using the eigen frequency of the structure as a mechanical input data can help find easier solutions, as did in this work.

The using of simplified-finite-element computer code allows the investigations to go much faster. As a comparison, calculations for all 6 Runs were made in 7 hours, while 2D codes took more than a week on a similar computer. This helps scientists to eliminate parameters to which the structure is less sensitive. But also permit new trends in the description of major mechanical sources.

This constitutes a new attempt to represent in a simplified manner, such type of structures, where it is important for dynamic shear mechanism to be well described.

REFERENCES

1. Mazars, J. & al. 1995. Analysis of the seismic response of R.C. structures using a multilayered F.E. model with damage concept. *Proceedings 5th SECED conference "European Seismic Design Practice"*: Chester UK.
2. La Borderie, C. 1991, Phénomènes unilatéraux dans un matériau endommageable : modélisation et application à l'analyse de structures en béton, Ph.D. memoir LMT Cachan - Université Paris 6, France.
3. Timoshenko, S.P. & Goodier J.N. 1970, Theory of elasticity, Mac Graw-Hill int. edit, chapter 2.
4. Crisfield, M.A. 1984, The application of shear-constraint to the generation of plate-elements, in f.e. methods for plate and shell structures, T.J.R. Hyghes and E. Hinton, vol. 1, pp 153-175.
5. Dubé J.F. 1994, Modélisation simplifiée du comportement visco-endommageable des structures en béton armé. Application aux séismes et aux chocs des structures. Doctoral Thesis at ENS Cachan.
6. Bathoz, J.L. & Dhatt, G. 1990, Modélisation des structures par éléments finis, édition Hermès, vol. 1 et vol. 2, pp. 61-93.
7. Seismic shear wall ISP - NUPEC's seismic ultimate dynamic response test. Comparison report, NEA/CSNI/R(96)10. OECD Nuclear energy agency, France.